Theoretical model and quantification of reflectance photometer

Lihua Huang (黄立华)[1,2*], Youbao Zhang (张友宝)[1], Chengke Xie (谢承科)[1,2], Jianfeng Qu (屈建峰)[1], Huijie Huang (黄惠杰)[1], and Xiangzhao Wang (王向朝)[1]

[1]*Shanghai Institute of Optics and Fine Mechanics, Chinese Academy of Sciences, Shanghai 201800, China*

[2]*Graduate University of Chinese Academy of Sciences, Beijing 100049, China*

[*]*E-mail: hlh@siom.ac.cn*

Received December 31, 2008

The surface morphology of lateral flow (LF) strip is examined by scanning electron microscope (SEM) and the diffuse reflection of porous strip with or without nanogold particles is investigated. Based on the scattering and absorption of nanogold particles, a reflectance photometer is developed for quantification of LF strip with nanogold particles as reporter. The integration of reflection optical density is to indicate the signals of test line and control line. As an example, serial dilutions of microalbunminuria (MAU) solution are used to calibrate the performance of the reflectance photometer. The dose response curve is fitted with a four-parameter logistic mathematical model for the determination of an unknown MAU concentration. The response curve spans a dynamic range of 5 to 200 μg/ml. The developed reflectance photometer can realize simple and quantitative detection of analyte on nanogold-labeled LF strip.

OCIS codes: 160.4236, 290.4020, 120.3890.

doi: 10.3788/COL20090711.1031.

In the past several decades, nanogold particles were popularly used as labels in many common immunoassays, e.g., sol particle immunoassay[1], flow cytometer, dot immunogold staining[2], immunoblotting[3], dot immunogold filtration assay[4], etc. During immunobiologic reaction, protein was adsorbed and coated by nanogold particles due to static effect. Gold labeled lateral flow (LF) assay has been investigated extensively due to the advantages of sensitivity, simplicity, and rapid response[5,6]. In this letter, the scattering and absorption behaviors of nanogold particles are analyzed based on Mie's theory, and the diffuse reflection of LF strip is investigated. Besides, a reflectance photometer is developed for LF strip labeled by nanogold particles. As an example, serial dilutions of microalbunminuria (MAU) are used to calibrate the reflectance photometer.

For spherical particles of any size, a general theory of light scattering and absorption was developed by Mie almost one century ago. The absorption and scattering characteristics of spherical particles depend on their shapes, sizes, surrounding media, etc.[7−10] Figure 1 shows the calculated absorption efficiency factor $Q_{\rm abs}$ and scattering efficiency factor $Q_{\rm sca}$ for a gold particle (about 60 nm in diameter) in water. The optical constants of nanogold particles referred to values of complex refractive index in bulk obtained from Weaver *et al.*[11] The peak wavelength (resonance wavelength) of $Q_{\rm abs}$ and $Q_{\rm sca}$ is about 540 nm, where $Q_{\rm abs}$ is about three times higher than $Q_{\rm sca}$.

The carrier of LF reaction – the LF strip, is composed of a sample pad, a conjugate pad, an analytical membrane, and an absorbent pad, as shown in Fig. 2. The analytical membrane was provided with an analyte-specific antibody capture line (test line; T line) and a species-specific antibody line (control line; C line)[12,13]. The T line and C line were in the center of the scanning window. The sampling hole was just on the top of the sample pad. Firstly, the aqueous sample was dropped into the sampling pad. Then the aqueous sample migrated via capillary action along the membrane, reaching T line and C line. Due to the immunoreactions between antibody and antigen, a certain amount of nanogold particles was attached on T line and C line. Because of the distinctive scattering and absorption of nanogold particles, the diffuse reflection of T line and C line was different from that of other regions of the LF strip. Besides, the diffuse reflection signal of T line was related to the concentration of analyte. The diffuse reflection signal of C line was to serve as a control for LF reaction regardless of the absence or presence of analyte. For convenience, we defined T line and C line as the functional region, and the other regions of the strip as the non-functional region.

The surface morphology of the strip was observed by a scanning electron microscope (SEM, 6360LA, JSM), as shown in Fig. 3. As seen from the SEM image, the strip was composed of the intersecting fibers, which constructed many pores with different sizes, and resulted in a rough surface of the strip. Here, the rough and porous strip was regarded as a nearly ideal diffuse reflector.

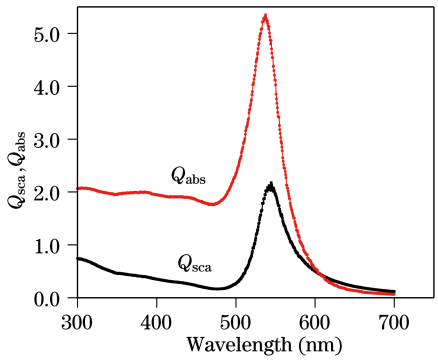

Fig. 1. Calculated scattering and absorption coefficients for homogeneous spherical gold particle with the radius of 30 nm in water.

 © 2009 Chinese Optics Letters

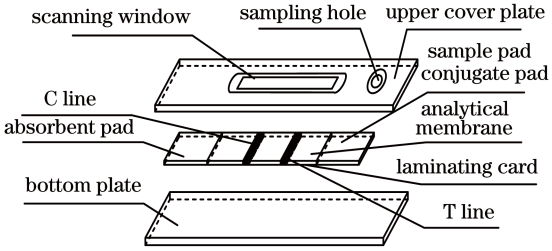

Fig. 2. Schematic illustration of the gold labeled LF strip.

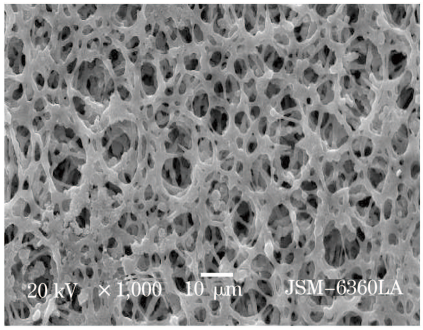

Fig. 3. SEM image of test strip surface.

When the non-functional region of the strip, where nanogold particles are absent, is illuminated by a light beam, the scattered luminous flux of LF strip can be expressed as

$$\Phi'_{\text{sca\_strip}} = \Phi_{\text{i}}, \tag{1}$$

where Φ_{i} is the incident luminous flux, and $\Phi'_{\text{sca\_strip}}$ is the scattered luminous flux of the strip within the illuminating spot. The diffuse reflection collected by the optical system is written as

$$\Phi' = \alpha \cdot \Phi'_{\text{sca\_strip}} = \alpha \cdot \Phi_{\text{i}}, \tag{2}$$

where α is related to the aperture angle of the collecting optical system.

When the functional region of the strip is illuminated by a light beam, the incident energy will be dissipated in several modes: the scattering of the strip, the scattering of the nanogold particles, and the absorption of the nanogold particles. The law of conservation of energy yields

$$\Phi_{\text{i}} = \Phi_{\text{sca\_strip}} + \Phi_{\text{sca\_gold}} + \Phi_{\text{abs\_gold}}, \tag{3}$$

where $\Phi_{\text{sca\_strip}}$, $\Phi_{\text{sca\_gold}}$, and $\Phi_{\text{abs\_gold}}$ are the scattered luminous flux of the strip within the functional region, the scattered luminous flux, and the absorption luminous flux of nanogold particles, respectively. What can be detected by the optical system is the scattered luminous fluxes of the strip and nanogold particles. Equation (3) can be rewritten as

$$\begin{aligned}\Phi_{\text{sca\_strip}} + \Phi_{\text{sca\_gold}} &= \Phi_{\text{i}} - \Phi_{\text{abs\_gold}} \\ &= \Phi_{\text{i}} - N \cdot \varphi_{\text{abs\_gold}},\end{aligned} \tag{4}$$

where N is the number of nanogold particles, and $\varphi_{\text{abs\_gold}}$ is the scattered luminous flux of a single nanogold particle. So the more nanogold particles present in the sample, the less light is diffused by the strip.

The scattered luminous flux of the strip is angle-independent, and that of nanogold particles is angle-dependent. However, only limited scattered luminous flux can be captured by the optical system. Moreover, Q_{sca} is about three times lower than Q_{abs} at the resonance wavelength. That is to say, the scattered irradiance collected by the optical system would be ten to twenty times lower than that absorbed by nanogold particles. In order to simplify the theoretical model, the scattered irradiance of nanogold particles collected by the optical system could be omitted. The diffuse reflection collected by the optical system is expressed as

$$\begin{aligned}\Phi = \alpha \cdot \Phi_{\text{sca\_strip}} &= \alpha \cdot (\Phi_{\text{i}} - \Phi_{\text{abs\_gold}}) \\ &= \alpha \cdot (\Phi_{\text{i}} - N \cdot \varphi_{\text{abs\_gold}}).\end{aligned} \tag{5}$$

From Eqs. (1) and (5), we can deduce that because of the absorption of nanogold particles, the signal amplitude of the functional region is less than that of the non-functional region. Φ and Φ' are all independent of the angle between collecting optical module and the surface normal of LF strip, which hardly influences the final sensitivity of the reflectance photometer. What needs to be considered is the miniaturization of the whole volume and the simplicity of the structure.

The structural illustration of the reflectance photometer is shown in Fig. 4. The reflectance photometer was composed of optical system (including illuminating module and collecting module), scanning system, photoelectric conversion and preamplifier system, data acquisition and control system.

The illuminating module was composed of the excitation source and the focusing lens. A 532-nm laser diode (LD) was selected as the excitation source. A cylindrical lens (focal length: 32.75 mm) was introduced to focus the beam to a nearly rectangular spot (i.e., a focal line) on the strip, parallel to the length axis of C line and T line. The size of the rectangular spot was 4× 0.02 (mm). The illuminating module was tilted at an angle of 45° relative to the LF strip surface, and the collecting module was vertical to the strip surface. The diffused light from the LF strip was firstly collimated by a collimating lens (focal length: 20.6 mm) with a numerical aperture (NA) of 0.4 and then focused on the rectangular slit by a focusing lens (focal length: 20.6 mm). The focused light through the slit entered a photodiode (PD). The electronic signal from PD was filtered and amplified,

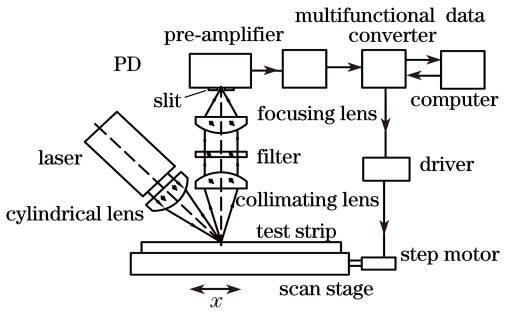

Fig. 4. Structural illustration of the reflectance photometer based on one dimensional scanning technology.

and then acquired with an embedded computer via a multifunctional data converter.

The scanning system was composed of the micro stepper motor, the motor driver, and the linear translation stage. The stage holding the LF strip was driven by the micro stepper motor to move in one dimension under the control of the embedded computer. The moving (or scanning) direction was vertical to the length axis of the rectangular spot. The scanning range and sampling resolution of stage were 10 mm and 20 μm, respectively, and totally 500 data points were obtained when the scanning process finished. The detection of the reflectance photometer could be completed within 1min (including the scanning time of 30 s and the information setting time of 30 s).

Figure 5 shows the signal distribution along the LF strip. Due to the absorption of nanogold particles of T line and C line, there existed two sunken regions. Such experimental result is consistent with the theoretical analysis. The reflection optical density of total sampling points within T line was integrated to indicate the signal value of T line. It yields

$$T(\mathrm{od}) = \sum \log_{10} \frac{V_0}{V_1}, \tag{6}$$

where V_1 is the signal value of the sampling point, and V_0 is the corresponding baseline signal value (Fig. 5). The baseline of T line could be deduced from its left and right boundary points. The integration of reflection optical density of C line, $C(\mathrm{od})$, could be obtained in the same way. The ratio $T(\mathrm{od})/C(\mathrm{od})$ is used as the final test result of one given LF strip.

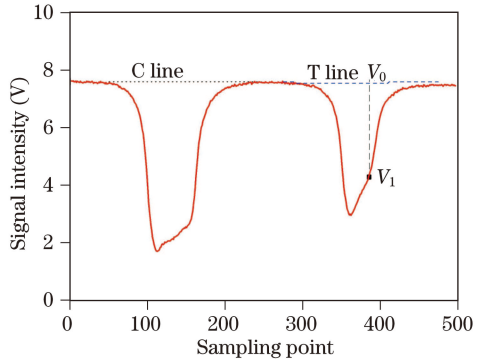

Fig. 5. Signal distribution along the LF strip.

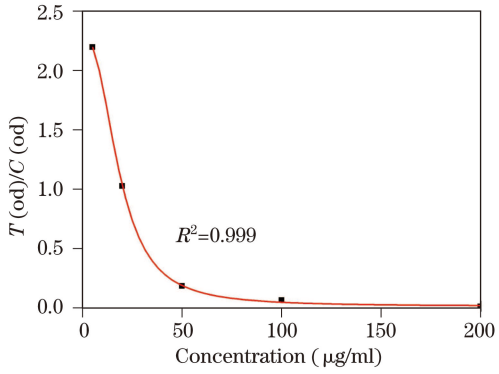

Fig. 6. Relation between the signal and the concentration of MAU.

We take the quantification of MAU solution for example to study the calibration of the reflectance photometer. MAU is an important marker of diabetes, cardiovascular disease, and hypertension in clinic medicine[14–16]. On LF strip, the binding of the MAU with nanogold-antibody inhibits the binding of nanogold-antibody with albumin on the T line. So the higher the concentration of MAU is, the less the nanogold particles are bound on T line. Five dilutions of pure cultures of MAU from 5 to 200 μg/ml were tested to deduce the standard quantitative equation of MAU detection. The signals are plotted against the concentrations for the dose response curve, as shown in Fig. 6. The dose response curve, which spanned a dynamic range of 5–200 μg/ml for MAU, could be described by four-parameter logistic (4PL) model[17,18]. The quantitative equation with the concentration as x and the signal of MAU as y is deduced as

$$y = 0.0168 + \frac{2.281 - 0.0168}{1 + (\frac{x}{18.314})^{2.479}}. \tag{7}$$

In actual quantitative detection, the signal of an unknown sample is put into the equation to obtain the MAU concentration.

In conclusion, the scattering and absorption behaviors of nanogold particles are analyzed based on Mie's theory. The diffuse reflection of porous LF strip with or without nanogold particles is investigated. Based on the theoretical analysis, a reflectance photometer is developed for LF strip with nanogold particles as reporter. The high accuracy micro stepper motor and linear stage provide one-dimensional scanning with the resolution of 20 μm. The 20-μm-wide slit is applied to reject stray light. The integration of reflection optical density is used to indicate the signals of T line and C line. Serial dilutions of MAU solution are employed to calibrate the reflectance photometer. The dose response curve and the quantitative equation are obtained with 4PL model. The developed reflectance photometer could realize simple quantitative detection of nanogold-labeled LF strip.

References

1. J. H. W. Leuvering, P. J. H. M. Thal, M. van der Waart, and A. H. W. M. Schuurs, J. Immunoassay Immunochem. **1,** 77 (1980).
2. G. J. Gray, R. Kaul, R. Sherburne, and W. M. Wenman, J. Bacteriol. **172,** 3524 (1990).
3. M. Wasowicz, S. Viswanathan, A. Dvornyk, K. Grzelak, B. Kłudkiewicz, and H. Radecka, Biosens. Bioelectron. **24,** 284 (2008).
4. Q. Huang, X. Lan, T. Tong, X. Wu, M. Chen, X. Feng, R. Liu, Y. Tang, and Z. Zhu, J. Clin. Microbiol. **34,** 2011 (1996).
5. E. I. Laderman, E. Whitworth, E. Dumaual, M. Jones, A. Hudak, W. Hogrefe, J. Carney, and J. Groen, Clin. Vaccine Immunol. **15,** 159 (2008).
6. A. Yu Kolosova, S. De Saeger, L. Sibanda, R. Verheijen, and C. Van Peteghem, Anal. Bioanal. Chem. **389,** 2103 (2007).
7. R. H. Doremus and P. Rao, J. Mater. Res. **11,** 2834 (1996).
8. C. F. Bohren and D. R. Huffman, *Absorption and Scattering of Light by Small Particles* (Wiley, New York, 1983).

9. X. Qu, J. Liang, C. Yao, Z. Li, J. Mei, and Z. Zhang, Chinese J. Lasers (in Chinese) **34,** 1459 (2007).
10. X. Qu, J. Wang, C. Yao, and Z. Zhang, Chin. Opt. Lett. **6,** 879 (2008).
11. J. H. Weaver and H. P. R. Frederikse, *Handbook of Chemistry and Physics* (CRC Press, Boca Raton, 1994).
12. S. Qian, and H. H. Bau, Anal. Biochem. **322,** 89 (2003).
13. S. Qian, and H. H. Bau, Anal. Biochem. **326,** 211 (2004).
14. A. R. Dyer, P. Greenland, P. Elliott, M. L. Daviglus, G. Claeys, H. Kesteloot, H. Ueshima, and J. Stamler, Am. J. Epidemiol. **160,** 1122 (2004).
15. P. Clausen, J. S. Jensen, G. Jensen, K. Borch-Johnsen, and B. Feldt-Rasmussen, Circulation **103,** 1869 (2001).
16. C. D. A. Stehouwer, M.-A. Gall, J. W. R. Twisk, E. Knudsen, J. J. Emeis, and H.-H. Parving, Diabetes **51,** 1157 (2002).
17. R. A. Dudley, P. Edwards, R. P. Ekins, D. J. Finney, I. G. M. McKenzie, G. M. Raab, D. Rodbard, and R. P. C. Rodgers, Clin. Chem. **31,** 1264 (1985).
18. P. B. Daniels, Clin. Chem. **40,** 513 (1994).